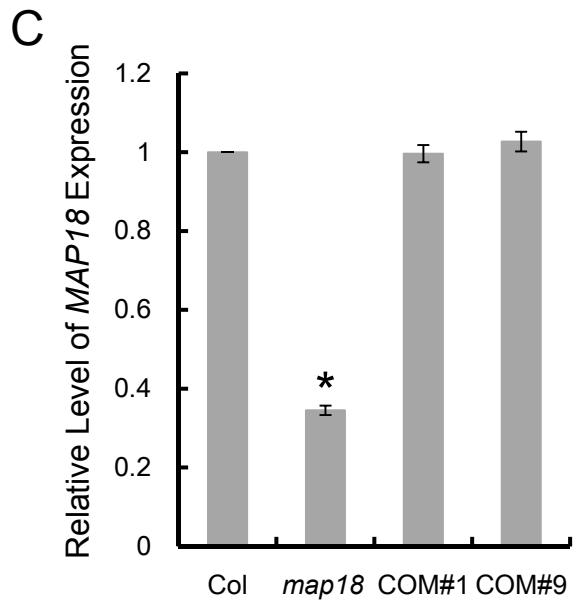
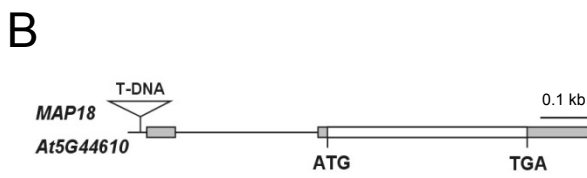
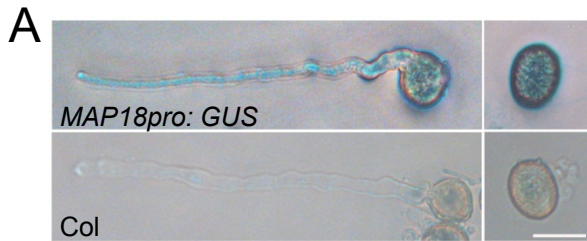


## Supplemental Figure 1



**Supplemental Figure 1.** *MAP18* Expression in Pollen and Pollen Tubes.

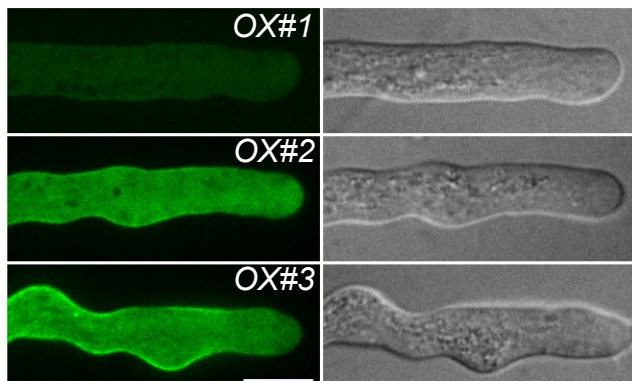
**(A)** Analysis of *MAP18* expression patterns using *MAP18**promoter*:*GUS* fusions. GUS activity was detected in pollen grains and pollen tubes. Bar = 20  $\mu$ m.

**(B)** Schematic view of the genomic structure of *MAP18* and the site of the T-DNA insertion. The white box represents the coding region, gray boxes represent exonic noncoding regions, and the line represents the intron. The T-DNA insert (open triangle) is located in the promoter region of *MAP18*.

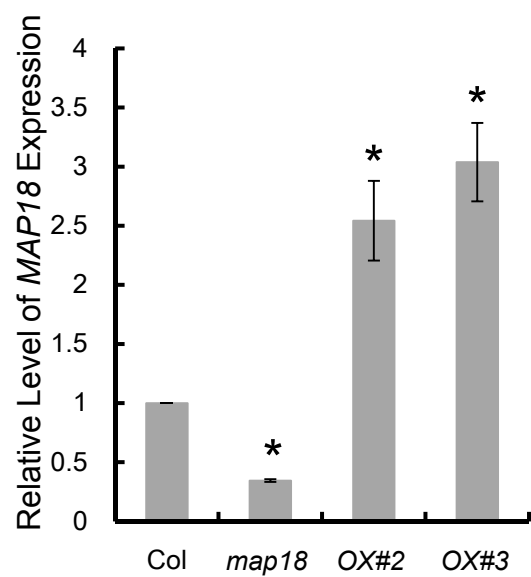
**(C)** The qRT-PCR analysis demonstrated that *MAP18* transcripts were significantly decreased in the *map18* mutant. The relative expression level of *MAP18* in the two complemented lines was similar to that of the wild type. Data represent the mean  $\pm$  SD. Relative amounts of gene expression were normalized to those of EF1 $\alpha$ . \* $p < 0.05$  by Student's *t*-test.

## Supplemental Figure 2

A



B



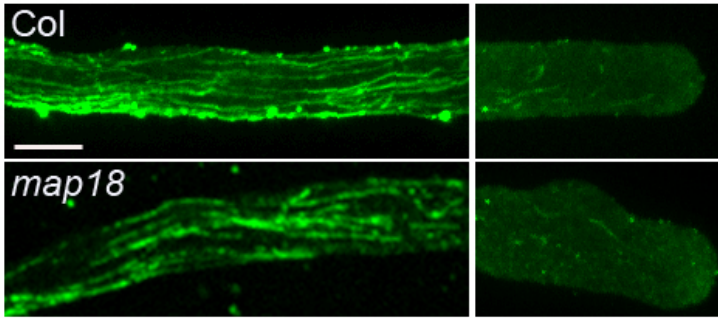
**Supplemental Figure 2.** Pollen Tube Growth Patterns Correlate with MAP18-eGFP Expression.

**(A)** The severity of the wavy-tube phenotype correlates with the fluorescence level of each MAP18-eGFP pollen tube. All images were collected under the same microscope setting.

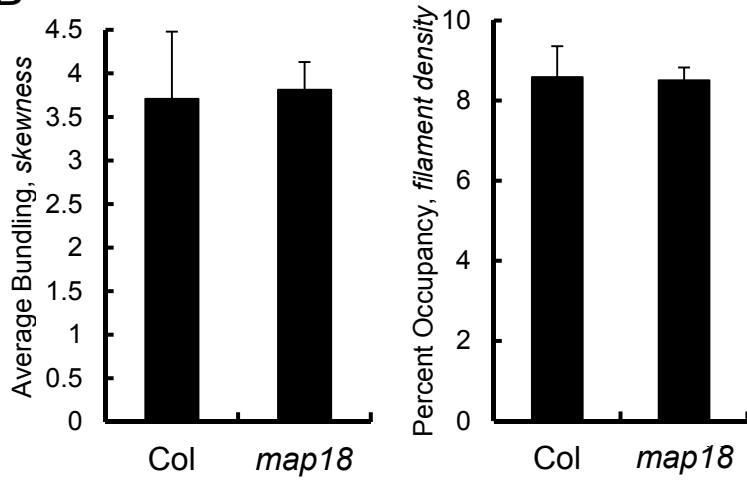
**(B)** The qRT-PCR analysis showed that the relative transcript level of *MAP18-eGFP* in transgenic lines #2 and #3 exceeded that in wild-type plants. Data represent mean  $\pm$  SD from at least three repeats. Relative amounts of gene expression were normalized to those of EF1 $\alpha$ . \* $p < 0.05$  by Student's *t*-test.

### Supplemental Figure 3

A



B

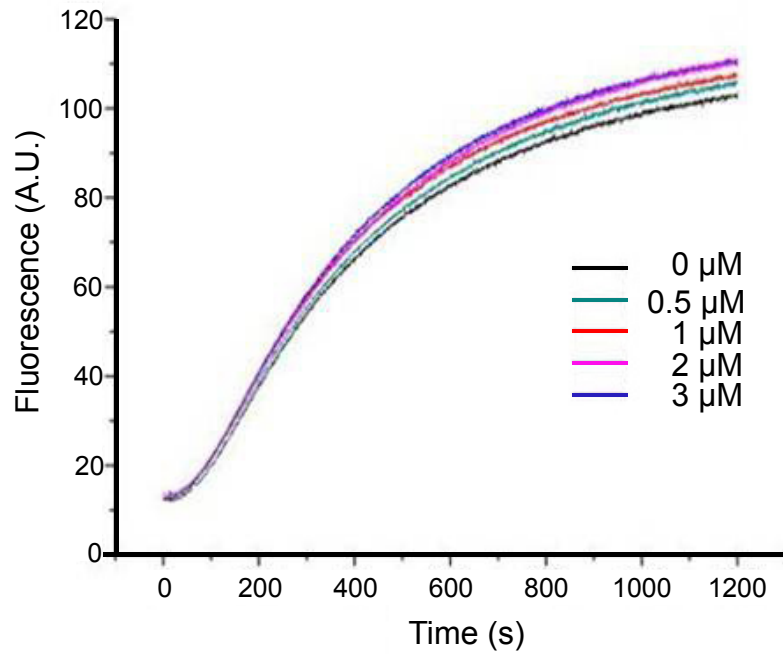


**Supplemental Figure 3.** Immunofluorescent Labeling of Microtubules in Pollen Tubes.

**(A)** Microtubules are organized as bundles along the elongation axis of the shank region. Few microtubules are detected in the apical domains of wild-type or *map18* pollen tubes. All images are projections of Z-stacks. Bar = 10  $\mu\text{m}$ .

**(B)** Quantification of microtubule organization in wild-type and *map18* pollen tubes. There is no significant difference in terms of microtubule bundling (indicated by the average skewness value) or percent occupancy of microtubules (indicated by the average filament density) between *map18* pollen tubes and wild-type pollen tubes. Data represent mean  $\pm$  SD from at least three repeats,  $p > 0.5$  by Student's *t*-test.

## Supplemental Figure 4

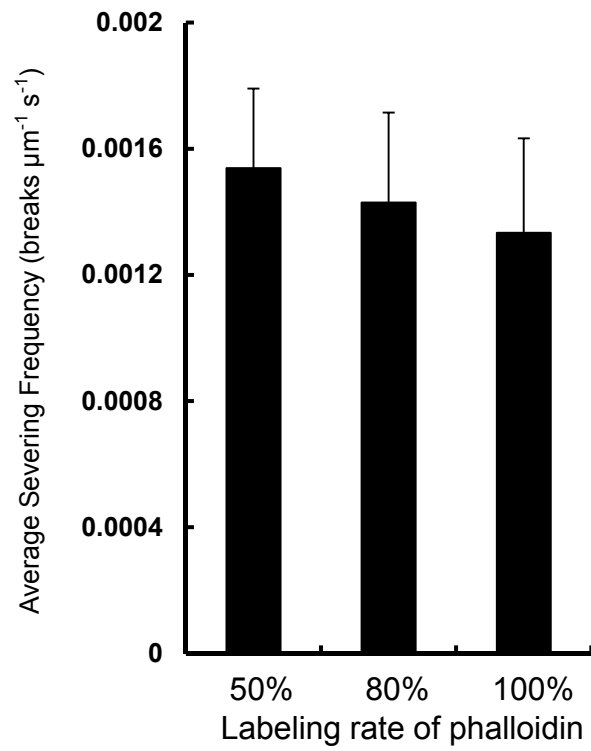


**Supplemental Figure 4.** Recombinant GST-MAP18 Has No Influence on Actin Polymerization.

An actin polymerization assay was performed using a G-actin solution with 5% pyrenyl-labeled actin in the presence of various concentrations of recombinant MAP18. The polymerization rate and the quantity of F-actin at equilibrium were unaffected by the presence or absence of GST-MAP18. The time course of actin polymerization was recorded by measuring pyrenyl fluorescence (A.U., arbitrary units).



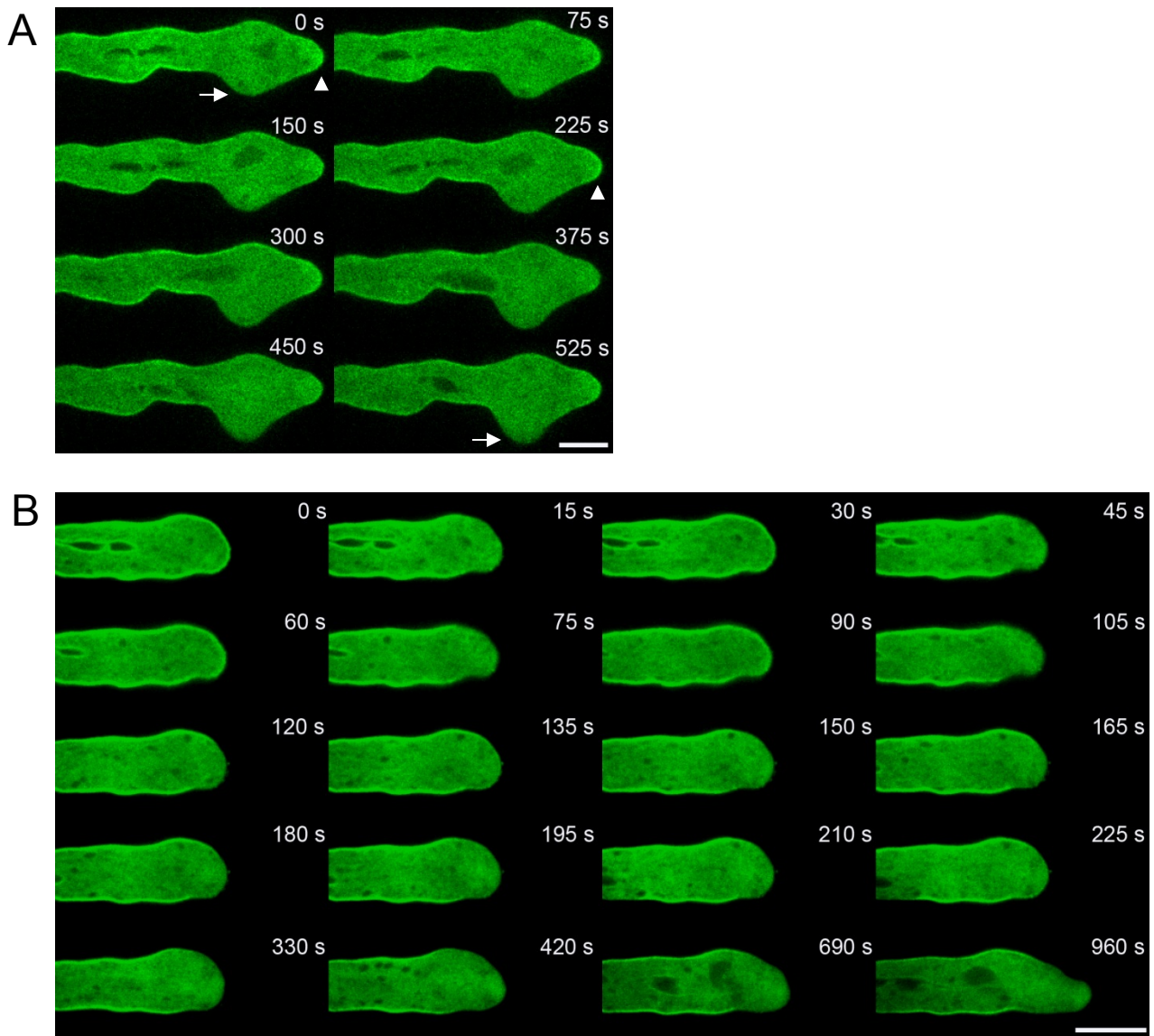
## Supplemental Figure 5



**Supplemental Figure 5.** Phalloidin Has No Negative Effect on F-actin  
Severing Activity of MAP18.

F-actin-severing frequencies by 10 nM MAP18 were not significantly altered by various concentration of phalloidin (in the presence of 50  $\mu\text{M}$   $\text{Ca}^{2+}$ ). Data represent mean  $\pm$  SD from three biological replicates. At least 15 filaments were examined for each experiment.

## Supplemental Figure 6

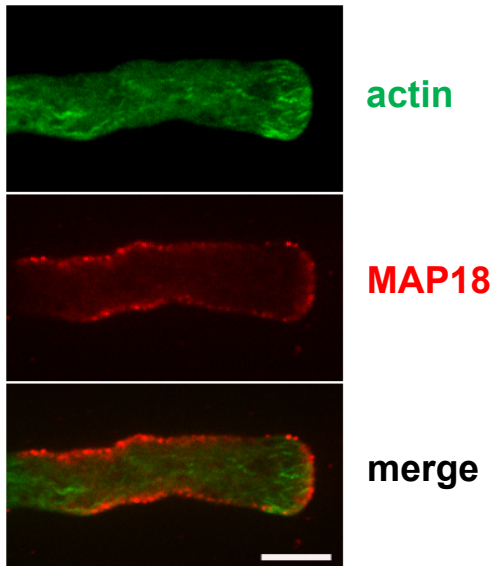


**Supplemental Figure 6.** The association of MAP18 with the Apical Plasma Membrane Is Related to the Cessation Growth of Pollen Tube Growth.

**(A)** Time course of a non-growing pollen tube expressing MAP18-eGFP recorded using spinning disc confocal microscopy. At beginning of our observation (defined as the time 0 s), MAP18-eGFP accumulates at the flank and apical plasma membrane (arrowhead), but disappears from another site at the subapical region (arrow) where the tube resumes its growth. Bar = 10  $\mu$ m.

**(B)** Time-lapse images taken from Supplemental Movie 5, showing oscillation of MAP18-eGFP in the apex as a pollen tube resumes growth. Pollen tubes were frozen at -20°C for 20 min to quickly terminate growth and then were transferred to room temperature and observed immediately (defined as the time 0 s) by spinning disc confocal microscopy. The MAP18-eGFP fluorescence signal at the apical plasma membrane was detected initially, but disappeared from the apical plasma membrane when pollen tube growth recovered. Bar = 10  $\mu$ m.

## Supplemental Figure 7



**Supplemental Figure 7.** Immunostaining by Anti-MAP18 Antibody Confirms the Plasma Membrane Localization Pattern of MAP18.

Immunostaining of MAP18 in a non-growing fixed pollen tube using anti-MAP18 antibody (red). The result showed that MAP18 was indeed localized to the plasma membrane in *Arabidopsis* pollen tubes. F-actin was visualized by Alexa488-phalloidin staining (green).

Bar = 5  $\mu$ m.

## Supplemental Figure 8

A

```

          10      20      30      40      50      60
MAP18x0  -----EKKKEEAKPVEVPVLA--E
RvCaBx2  ----PVEVITKDLPEVEEAP----AAVEEESKTEEVVEPKKEEVEETKTEETPAVVEE-E
PCaP1x1  MGYWNSKVVPKFKKLFKNSAKKAAAAEATKTFDESKETINKEIEEKKTELQPKVVETYE
          :: ** * . * : . *
Prim.cons. MGYW222V22K22222E22SAKKA22E22KT22222222EE3EE3KTEE3P3VVE3YE

          70      80      90      100     110     120
MAP18x0  EKKPAVEEKKKTAPEVEEKK-----
RvCaBx2  SKTEEVVEPKKEEVEETKT-----
PCaP1x1  ATSAEVKALVRDPKVVAGLKKNSAAVQKYLEELVKIEFPGSKAVSEASSSFGAGYVAGPVT
          . . * : * * *
Prim.cons. 3K33EV3E3KK333VEE3K2NSAAVQKYLEELVKIEFPGSKAVSEASSSFGAGYVAGPVT

          130     140     150     160     170     180
MAP18x0  -----PAVEEEK-----KPAVEEKKP--VEE-----KKE-----VVAAPVVA
RvCaBx2  ---EETPAVVEEESKAEDVVEPKKEEETPAVVEEESKTEEVVEPKKEEAPVVEEETKA
PCaP1x1  FIFEKVSVFLPEEVVTKTEIPVEEVKAEPAKTEEPAKTEGTSGEKEE-----IVEETKKG
          . . . * : * * * . . . * . . . * : * . . . *
Prim.cons. FIFE22PAV3EEE2K222223P3VEE3PA2VEE2KTE22222KKEEAPVVEE33KA

          190     200     210     220     230
MAP18x0  ETPSTKAPETPVVETPAKAPET-----PAAAP-----QKA--
RvCaBx2  EEEVKKTEETPAVVEEKKPEAESEEKTEVAAVQAAAAPAEVAVEKADE
PCaP1x1  ETPETAVVEEKKPEVEEKKKEEATPAPAVVETPVKEPETTTTAPVAEPPKP
          * . . * * * * : * : . . . . . . . . . .
Prim.cons. ETP3TK33ETP3VE3EEKKPEA222222E22222PAAAP22222EKA22
    
```

B

```

MAP18  MGYWKSQVPRMKKLFKSPAKKEVVEEKKPREVEVVEE.....VVVKT.....EPPAKEGETKPEEII 59
AtVLN3  MSGSTKVLDPAFQGVGQKPGTEIWRIENFEPVVPKSEHGKFYMGDITYIVLCTTQNKGGAYLFDIHFWIGKDTSQDEAGTAAVKTVELDA 90
ABP29  MANSSKNLDEAFQGVGQRLGTEIWRIENFQVSLPKSDHGKFSYSGDSYIVLCTTAGKGGAHLYDIHFWIGKDTSQDEAGTAAIKTVELDA 90
Consensus  m      p      e      p      v      t      e      e
MAP18  ATGEKEIEIVVEEKKFA.....KPEVEVPVLA--E..KPAVEEKKKTAPEVEEKKPAVEEKKPAVEE..... 120
AtVLN3  ALGGRAVQYREIQGHSDKFLSYFRFCIIPLEGGVASGFKRPEEDEFETRLTYCKGKRAVHLKQVFFARSSLNHDDVFIIDTKEKIYQFM 180
ABP29  VLGGRAVQYREIQGHSDKFLSYFRFCIIPLEGGVVSQKTEPEEETFETRLTYCRGKRVVRLKQVFFARTSLNHDDVFIIDTKEKIYQFM 180
Consensus  g      e      e      p      p      k      p      e      k      v      p
MAP18  ..KPEVEEKKPEVVAAPVVAETPSTKAPETPVVETPAKAPET.....PAAAPQKA..... 168
AtVLN3  GANSNIQDRAKALVVIQYLKDRFHEGTSQVAIVDDGKLDTESDSGEFWVLFGGFAPVARKVASEDEIIPETTPPRLYSIADGGQVESIDGD 270
ABP29  GANSNIQDRAKALEVIQFLKDRYHEGTCQVAIIDDGRLAAESGSGEFWVLFGGFAPVIGKRVVGGDDVTLETTPGRLY..... 257
Consensus  e      k      e
    
```

C

```

MGYWKSQVPRMKKLFKSPAKKEVVEEKKPREVEVVEE VVVK
                        1
TEPPAKEGETKPEEIIATGEKEIEIVVEEKKKEEAKPVEVPVLA--E
                        2
KPAVEEKKKTAPEVEEKKPAVEEKKKPAVEEKKKPEVEEKKKEVVA
        3         4         5         6         7
VPVAETPSTKAPETPVVETPAKATETPAAAPQKA
    
```

**Supplemental Figure 8.** PCR-Based Site-Directed Mutagenesis.

**(A)** Multiple alignment and analysis of amino acid sequences of MAP18, *Arabidopsis* PCaP1, and *Raphanus sativus* RVCaB using CLUSTALW ([http://npsa-pbil.ibcp.fr/cgi-bin/npsa\\_automat.pl?page=/NPSA/npsa\\_clustalw.html](http://npsa-pbil.ibcp.fr/cgi-bin/npsa_automat.pl?page=/NPSA/npsa_clustalw.html)).

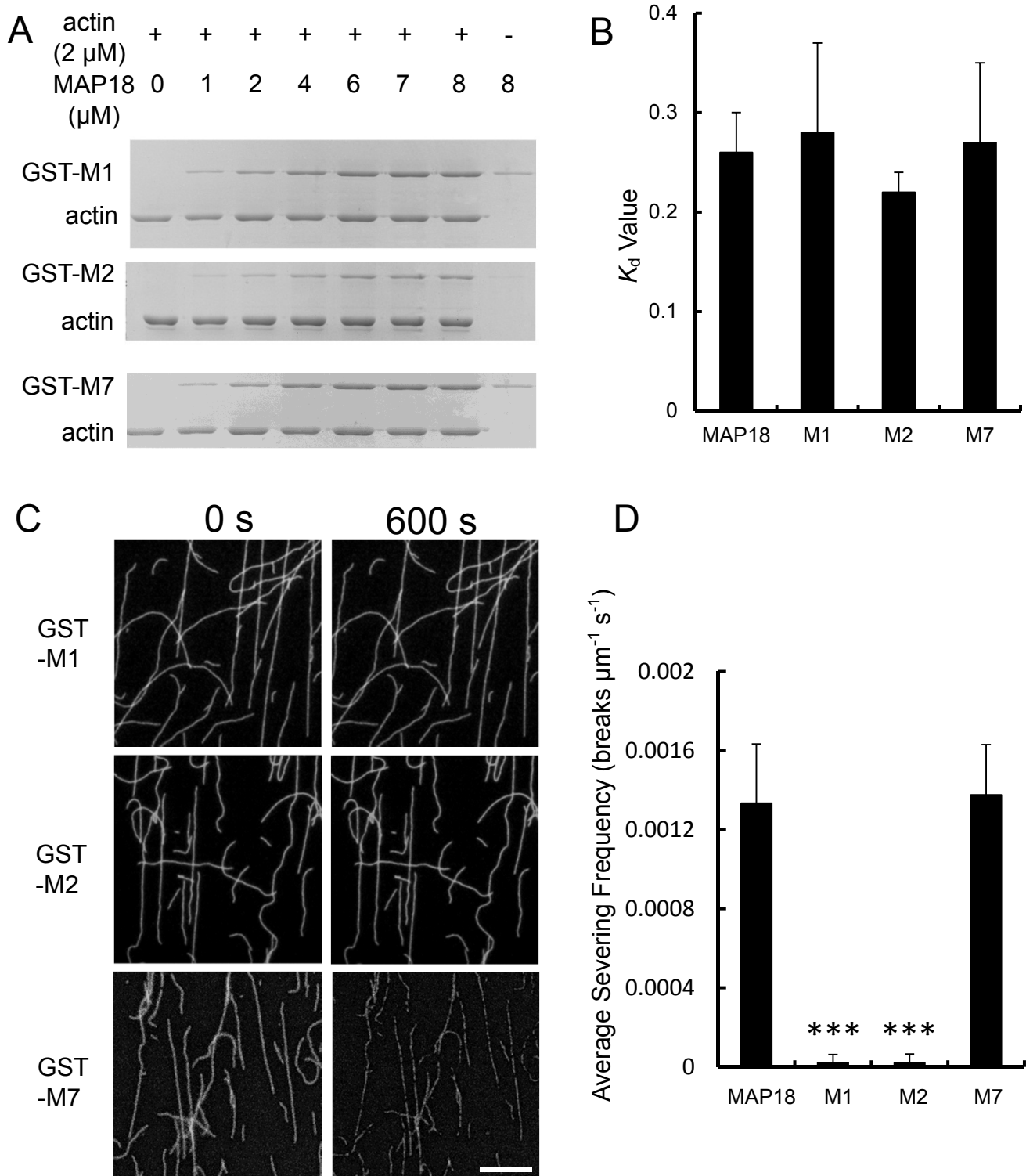
High contents of glutamate, lysine, and valine residues were common in MAP18, PCaP1, and RVCaB sequences, which contain seven, four, and nine repeats, respectively, of the VEEKK motif (with some variation). (\*) residues in red font are identities, (:) residues in green font are strong similarities, (.) residues in blue font are weak similarities. Similar sequences are coincident with the VEEKK motif.

**(B)** Multiple alignment and analysis of amino acid sequences of MAP18, *Arabidopsis* VILLIN3, and *L. longiflorum* ABP29. The latter two proteins sever actin filaments in the presence of  $\text{Ca}^{2+}$ . Charged glutamate and lysine residues are relatively conserved among MAP18, VILLIN3, and ABP29. Residues highlighted in dark blue are identities.

**(C)** MAP18 protein mutants generated by PCR-based site-directed mutagenesis within repeated VEEKK motifs. Seven imperfect VEE(N)K repeats in the amino acid sequence of MAP18 are shown in red and underlined as 1 – 7. E (Glu) and K (Lys) in green correspond to sites that are essential for F-actin-severing activity.



## Supplemental Figure 9



**Supplemental Figure 9.** F-Actin-Binding and -Severing Activities of MAP18 Mutant Proteins M1, M2, and M7.

**(A)** A co-sedimentation assay was performed to assess the binding of GST-M1/M2/M7 to actin filaments. All three mutant proteins bound to F-actin in vitro. Experiments were repeated at least three times and a representative result is shown in **(A)**.

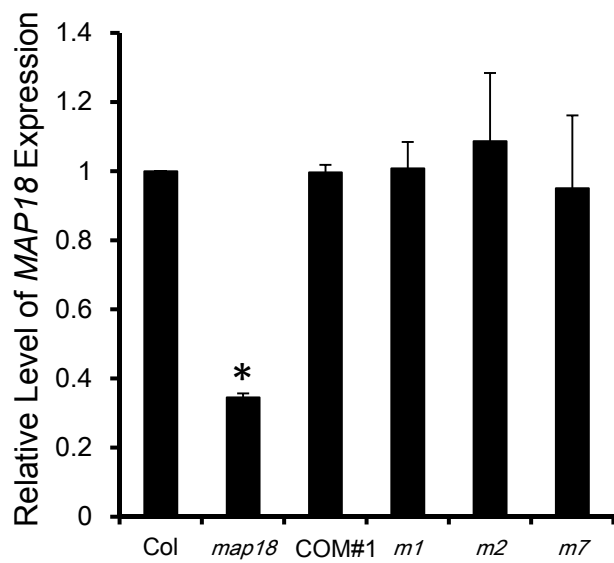
**(B)** The mean  $K_d$  values for the binding of MAP18 mutant proteins M1, M2, and M7 to actin filaments were obtained from three independent experiments. No significant difference in terms of the mean  $K_d$  value was detected between wild-type MAP18 protein with any mutant protein. Error bars indicate  $\pm$  SD.

**(C)** The severing activities of MAP18 mutants were observed directly by TIRFM (total internal reflection fluorescence microscopy). Pre-polymerized, Alexa 488-phalloidin-labeled actin filaments were incubated with M1, M2, or M7 in the presence of  $Ca^{2+}$ , and images were collected every 20 s. The representative images correspond to actin filaments at the start of observation and after 600 s. Significant breaks in individual actin filaments were observed following incubation with M7, but not M1 or M2.

Bar = 10  $\mu$ m.

**(D)** Quantitative analysis of severing frequency confirmed that M7 retained the F-actin severing activity just as the wild-type MAP18 in the presence of 50  $\mu$ M  $Ca^{2+}$ . However, the F-actin severing activity of M1 and M2 mutant proteins was dramatically reduced. Data represent mean  $\pm$  SD from three repeats. At least 15 filaments were examined in each experiment. \*\*\* $p < 0.001$  by Student's  $t$ -test.

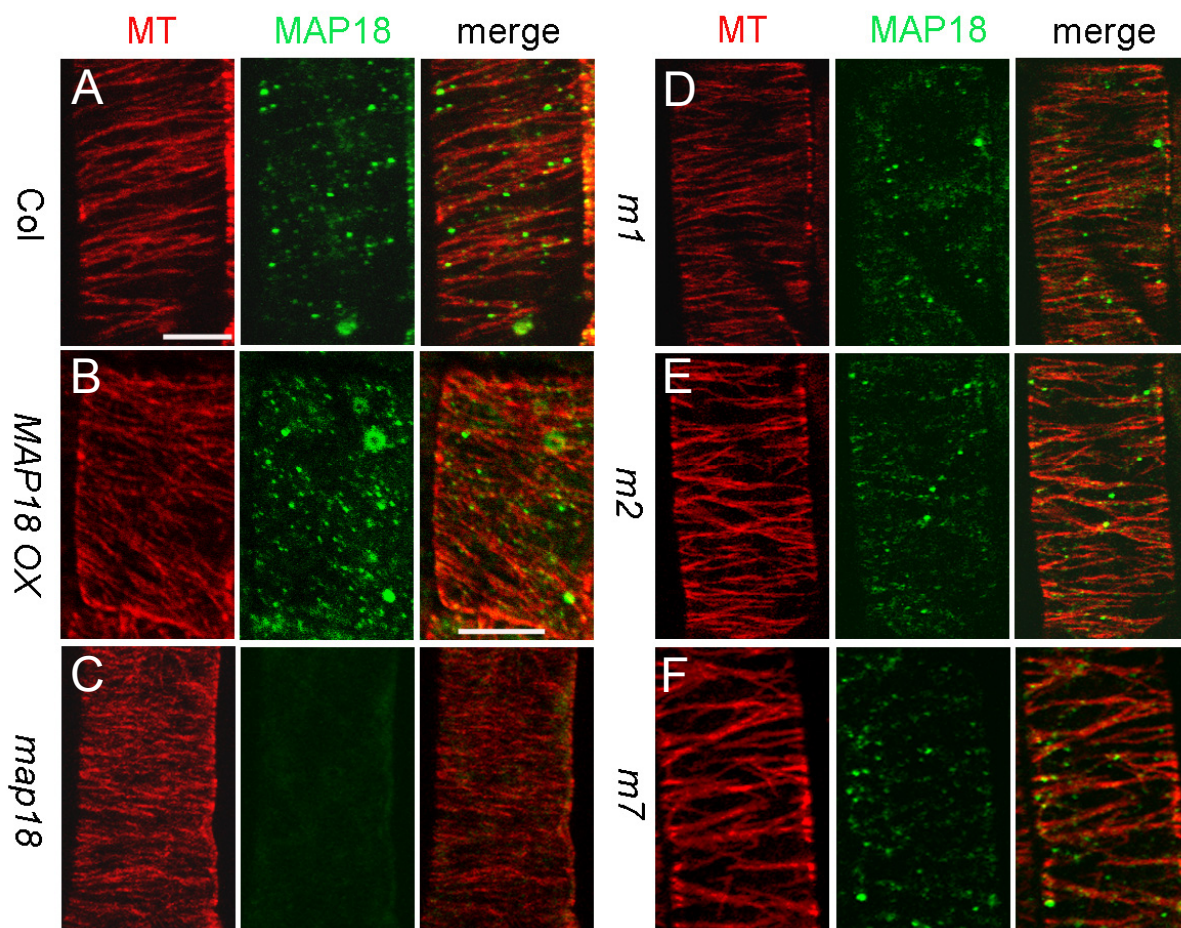
## Supplemental Figure 10



**Supplemental Figure 10.** The qRT-PCR Analysis of the Transcript Levels of *MAP18* and *M1*, *M2* and *M7* in Various Transgenic Lines.

The relative transcript levels of *M1*, *M2* and *M7* in respective *m1*, *m2* and *m7* transgenic lines were similar to the expression level of *MAP18* in the wild type. Data represent the mean  $\pm$  SD from three biological replicates. Relative amounts of gene expression were normalized to those of EF1 $\alpha$ . \* $p < 0.05$  by Student's *t*-test.

## Supplemental Figure 11



**Supplemental Figure 11.** Immunofluorescence Microscopy Demonstrated That GFP-tagged MAP18 and Its Mutants (M1, M2, M7) Localized to Microtubules in Root Epidermal Cells.

**(A)** MAP18 partially colocalized with cortical MTs in wild-type root epidermal cells.

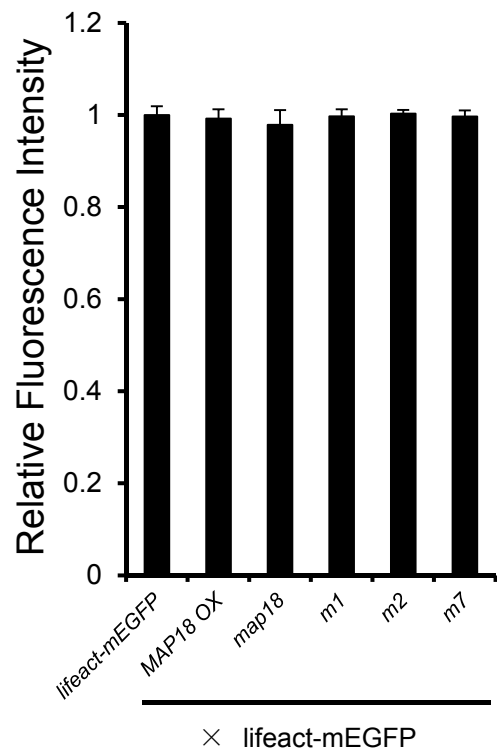
**(B)** MAP18-eGFP partially colocalized with cortical MTs in *MAP18 OX* root epidermal cells.

**(C)** Rarely any MAP18 signal was detected in *map18* root epidermal cells.

**(D) to (F)** M1-eGFP **(D)**, M2-eGFP **(E)**, and M7-eGFP **(F)** partially colocalized with cortical MTs in root epidermal cells.

GFP-tagged MAP18 and its mutant proteins were transformed into the *map18* mutant. Left panel: Cortical microtubules; middle panel: MAP18 proteins; right panel: merged images. Bar = 10  $\mu$ m.

## Supplemental Figure 12



**Supplemental Figure 12.** The Relative Fluorescence Intensity of Lifeact-mEGFP Probes in Various Plants.

*Arabidopsis* line expressing *Lat52:lifeact-mEGFP* was crossed to the *map18* mutant and *MAP18 OX*, *m1*, *m2*, *m7* transgenic plants. Lines that displayed similar fluorescence intensity as the *Lat52:lifeact-mEGFP* line under the same microscope settings were chosen for further analysis. Error bars indicate  $\pm$  SD.



**Supplemental Table 1.** Mutated Positions and Primer Information for Seven Site-Directed Mutants of MAP18.

|          | Mutagenesis<br>in base | Mutagenesis in<br>amino acid<br>residues | Pairs of specific primers                           |
|----------|------------------------|--|---|
| MAP18-M1 | 169A→C                 | 27E→A                                    | F:AAGTTGTT <b>GCGGAGGAGCG</b> CCACGAGAGGTGGAA       |
|          | 177A→G                 | 30K→A                                    | R:CCTTTTTTGCTGGACTCTTCTCG                           |
|          | 178A→C                 |  |   |
| MAP18-M2 | 298A→G                 | 70E→G                                    | F:GTT <b>GGAGAGAAGGG</b> GAGAAGAGGCTAAACCGG         |
|          | 306G→A                 | 73K→G                                    | R:TATTCTATCTCTTTCTCGCCGG                            |
|          | 307G→A                 |  |   |
| MAP18-M3 | 373A→G                 | 95E→G                                    | F:AGCCAGCCGT <b>AGGAGAGGAGAAGGCG</b> ACG            |
|          | 384A→G                 | 99K→A                                    | R:TCTTCTCCTCCGACGTGCGA                              |
|          | 385A→C                 |  |   |
| MAP18-M4 | 400A→G                 | 104E→G                                   | F:GGT <b>GGAGAGAAGGCG</b> CCAGCTGTGGAAGAGGAGAAGAA   |
|          | 408A→G                 | 107K→A                                   | R:GGCGCCGTCTTCTCTCTTCTACGGCT                        |
|          | 409A→C                 |  |   |
| MAP18-M5 | 422A→G                 | 111E→G                                   | F:CAGCTGT <b>GGAGGAGAGAAGGCG</b> CCTGCCGTGGAAGAGAA  |
|          | 432A→G                 | 114K→A                                   | R:GCTTCTTCTTCCACCGGCGCCGTCTTCTT                     |
|          | 433A→C                 |  |   |
| MAP18-M6 | 445A→G                 | 119E→G                                   | F:CCTGCCGT <b>GGAGAGAGAAGG</b> ACCTGTGGAGGAGGAGAAAA |
|          | 453A→G                 | 122K→G                                   | R:CTTCTTCTCTTCCACAGCTGGC                            |
|          | 454A→G                 |  |   |
| MAP18-M7 | 466A→C                 | 126E→A                                   | F:CCTGT <b>GGAGGCGGAGAAAGG</b> GAGAAGTTGTT          |
|          | 474A→G                 | 128K→G                                   | R:TTTCTTCTTCCACGGCAGG                               |
|          | 475A→G                 |  |   |

**Supplemental Table 2.** F-Actin-Binding and -Severing Activities of the Six MAP18 Protein Mutants.

| Name            | Mutant position | Binds F-actin | Severs F-actin<br>with Ca <sup>2+</sup> |
|-----------------|-----------------|---------------|---|
| MAP18 wild-type |                 | +             | +                                       |
| MAP18-M1        | 27E→A           | +             | -                                       |
|                 | 30K→A           |               |   |
| MAP18-M2        | 70E→G           | +             | -                                       |
|                 | 73K→G           |               |   |
| MAP18-M3        | 95E→G           | +             | +                                       |
|                 | 99K→A           |               |   |
| MAP18-M4        | 104E→G          | +             | +                                       |
|                 | 107K→A          |               |   |
| MAP18-M6        | 119E→G          | +             | +                                       |
|                 | 122K→G          |               |   |
| MAP18-M7        | 126E→A          | +             | +                                       |
|                 | 128K→G          |               |   |